SCALING LAWS FOR LARGE EARTHQUAKES
CONSEQUENCES FOR PHYSICAL MODELS

Christopher H. Scholz

Department of Geological Sciences and

Lamont-Doherty Geological Observatory

of Columbia University, Palisades, New York 10964

ABSTRACT

It is observed that the mean slip in large earthquakes correlates linearly with fault length L and is not related to fault width, W. If we interpret this in terms of an elastic model, it implies that static stress drop increases with aspect ratio (L/W). We also observe a tendency, particularly for strike-slip earthquakes, for aspect ratio, and hence static stress drop, to increase with seismic moment. Dynamic models of rupture of a rectangular fault in an elastic medium show that the final slip should be controlled by the fault width and scale with the dynamic stress drop. The only way these models can be reconciled with the observations is if dynamic stress drop correlates with fault length so that it is also nearly proportional to aspect ratio. This could only happen if fault length is determined by the dynamic stress drop. There are several serious objections to this, which lead us to suspect that these models may be poor representations of large earthquakes. Firstly, it conflicts with the observations for small earthquakes (modeled as circular sources) that stress drop is nearly constant and independent of source radius. Secondly,

it conflicts with the observation that fault length is often determined by rupture zones of previous earthquakes or tectonic complications. We speculate that the boundary condition at the base of the fault, that slip is zero, is unrealistic because that edge is in a ductile region at the base of the seismogenic layer. In a model in which slip is not so constrained at the base of the fault nor at the top (the free surface), such that no healing wave originates from these edges, final slip would be determined by fault length. The observations would then be interpreted as meaning that the static and dynamic stress drops of large earthquakes are nearly constant. These two alternatives predict very different scaling of the dynamics of large earthquakes. The width-dependent model predicts that average particle velocities are larger for long ruptures but the rise time will be the same as in a shorter event of the same width. The length-dependent model predicts the opposite.

INTRODUCTION

A central problem in earthquake seismology has been to find scaling laws that relate the static parameters such as slip and stress drop to the dimensions of the rupture and to understand these relationships in terms of the dynamic parameters, the most fundamental of which are rupture velocity and dynamic stress drop.

In doing so, it is essential to distinguish between small earthquakes and large earthquakes. Tectonic earthquakes nucleate and are bounded within a region of the earth between the surface and a depth h_o, the seismogenic layer. The seismogenic depth, h_o, depends on the tectonic environment but in a given region the maximum width of an earthquake occurring on a fault of dip δ is $W_o = h_o/\sin \delta$. We will define a small earthquake as one with a source radius $r \leq W_o/2$ and a large earthquake as one in which $r > W_o/2$. Thus a small earthquake can be represented as a circular source in an elastic medium, whereas a large earthquake is more suitably treated as a rectangular rupture with one edge at the free surface.

It has been repeatedly demonstrated (e.g., Aki, 1972; Thatcher and Hanks, 1973; Hanks, 1977) that the stress drops of small earthquakes are nearly constant and independent of source dimensions. This result, when interpreted with dynamic models of finite circular ruptures (Madariaga, 1976; Archuleta, 1976; Das, 1980), simply means that the dynamic stress drop is constant.

If the same were true for large earthquakes, the dynamic models of rectangular faulting in an elastic medium (Day, 1979; Archuleta and Day,

1980; Das, 1981) would predict that the mean slip is a linear function of fault width. In the next section we will show that this prediction is not borne out by the observations. What is observed instead is that slip correlates linearly with fault length. The principal point of this paper is to discuss the consequences of that observation for the physics of large earthquakes.

OBSERVATIONS

For small earthquakes, using the definition of seismic moment, M_o, and the relationship

$$\Delta\sigma = \frac{7\pi}{16}\mu\frac{\bar{u}}{r}$$

where r is source radius, $\bar{u}$ is mean slip, and $\Delta\sigma$ is stress drop. If stress drop is constant, the relationship between M_o and fault area, A, is

$$M_o = (\frac{16\Delta\sigma}{7\pi^{3/2}}) A^{3/2} \quad .$$ (1)

Large earthquakes, however, are more nearly rectangular ruptures of width W and length L and in this case, for an elastic model in which slip is restricted to be within W,

$$\Delta\sigma = C\mu\frac{\bar{u}}{W}$$ (2)

where C is a geometrical constant.

If stress drop were constant, we would expect to find that

$$M_o = \frac{\Delta\sigma}{C}LW^2$$ (3)

In Figure 1 we show a plot of log LW^2 vs. log M_o, for the large interplate thrust and strike-slip earthquakes from the data set of Sykes

and Quittmeyer (1981). These observations are listed in Table 1. The data for each type of earthquake define a line, but with a slope less than one, indicating that stress drop systematically increases with moment. The offset between the data for the strike-slip and thrust events is also an important feature that we will discuss later.

These data indicate that $\bar{u}$ is not simply related to W and that $\Delta\sigma$ is not constant for large earthquakes. On the contrary, many workers (e.g., Bonilla and Buchanan, 1970; Slemmons, 1977) have argued that $\bar{u}$ correlates with L, and recently Sykes and Quittmeyer (1981) have argued that the correlation is linear. Plots of $\bar{u}$ vs. L on linear scales are shown in Figures 2 and 3 for strike-slip and thrust earthquakes, respectively.

In view of the usual uncertainties in the estimates of $\bar{u}$ and L, and any naturally occurring variations in dynamic stress drop (with which slip should be expected to scale), the correlation between $\bar{u}$ and L is fairly strong. We fit it with a straight line with an intercept at the origin

$$\bar{u} = \alpha L \qquad\qquad (4)$$

and find that $\alpha \simeq 2 \times 10^{-5}$ for the thrust events and 1.25×10^{-5} for the strike-slip events. At least for the strike-slip events, slip is clearly not dependent on width because the widths of all the events in Figure 2 are between 10-15 km, i.e., they are essentially the same.

From this observation we would then expect that

$$M_o \, \propto \, \mu\alpha L^2 W \qquad\qquad (5)$$

which is confirmed in Figure 4. For reference, the line drawn through the data has a slope of one.

Since

$$L^2 W \equiv A^{3/2} (\frac{L}{W})^{\frac{1}{2}}$$

and since the aspect ratio L/W varies only by a factor of about 20 in the data-set, we would have found a good correlation between M_o and $A^{3/2}$, as did Aki (1972) and Kanamori and Anderson (1975) had we plotted log A vs. log M_o. The question is not whether M_o correlates better with $L^2 W$ than with $A^{3/2}$. The issue of concern is that Kanamori and Anderson's interpretation of their correlation as meaning that stress drop is constant is only true if L/W is constant, because from (2) and (4), we have

$$\Delta \sigma = C \mu \sigma \frac{L}{W} . \tag{6}$$

That L/W is a constant is an explicitly stated assumption of Aki (1967, 1972) and Kanamori and Anderson (1975), and although Abe (1975) and Geller (1976) attempted to observationally justify this assumption, it is not generally true. In Figures 5 and 6 we plot $\Delta \sigma$ vs. L/W for the two types of earthquakes. The correlation between them is very clear for the strike-slip events, and less so for the thrust events, for which there is a much smaller variation of aspect ratio. That L/W does not have a large variation for the thrust events seems to simply result from the fact that the seismogenic width of subduction zones, W_o, is about 100 km, so that only extremely large events can achieve high values of aspect ratio.

We can now understand why stress drop increases systematically with M_o, as shown in Figure 1. The width of large strike-slip earthquakes is

limited by the seismogenic depth to $W_o \gtrsim 15$ km so that they grow principally in the L direction. This results in a systematic increase in L/W, and hence $\Delta\sigma$, with M_o. The subduction zone thrust earthquakes have different widths but L increases faster than W with increasing moment, producing the same result, i.e., $\Delta\sigma$ increases with L/W or M_o. The offset between the data for thrust and strike-slip events in Figure 1 occurs simply because the widths of the thrust events are much greater than those of the strike-slip events. A strike-slip event must have a much greater aspect ratio, and hence stress drop, than a thrust event of the same moment.

PHYSICAL CONSEQUENCES

The principal feature of the observations that we wish to explain is the correlation between slip and fault length. It is a surprising observation because intuition would first lead one to expect slip to depend on width, yet this is not observed. This intuition is re-inforced by the results of dynamic models of rectangular faults in an elastic medium (Day, 1979; Archuleta and Day, 1980; Das, 1981). These models show that slip is controlled by the width of the fault and that it scales with dynamic stress drop.

The situation is illustrated in Figure 7, which shows surface slip along the fault for two representative strike-slip earthquakes. These earthquakes have essentially the same width, and differ only in length. If the dynamic stress drop were the same for these two earthquakes, then according to the theory, the Ft. Tejon earthquake would be the equivalent of six Mudurnu earthquakes placed end to end. Clearly that is not the case.

If the dynamic, elastic models are correct representations of earthquakes, then the only way they can be reconciled with the observations is if dynamic stress drop correlates with aspect ratio. Since the width of strike-slip events is nearly constant, and the width varies much less than length for the thrust events, this would be approximately true if dynamic stress drop correlates linearly with fault length. The only way this can happen without violating causality is if fault length is determined by dynamic stress drop. This is not an entirely unphysical proposition, because dynamic stress drop determines the stress intensity factor, which

is important in fracture growth. It is not obviously apparent, however, why L should increase linearly with $\Delta\sigma_d$, the dynamic stress drop.

There are several major objections to this interpretation. The first is that we have to assume that for large earthquakes $\Delta\sigma_d$ determines the rupture length, which directly contradicts the observations for small earthquakes. Although stress drop appears to increase with source radius over a limited range in some data sets (Aki, 1980), it shows no obvious variation with source radius over a very broad range (Hanks, 1977). We can offer no reasonable explanation for why large earthquakes should behave differently than small earthquakes in this important respect.

A second objection is that this assumption conflicts with the principal observations that led to the concept of seismic gaps: that the length of large earthquakes is often controlled by the rupture zones of previous earthquakes or by structural features transverse to the fault zone. Of course, one could soften the original assumption to: $\Delta\sigma_d$ determines the length unless the rupture encounters a rupture zone of a previous earthquake or a transverse feature. The rejoinder is that if the latter were as common as is thought, it would have the effect of destroying the correlation between $\bar{u}$ and L that is observed.

It is worth giving a specific example. If we compare the 1966 Parkfield earthquake (L = 30 km, $\bar{u}$ = 30 cm, W = 15 km) and the 1906 San Francisco earthquake (L = 450 km, $\bar{u}$ = 450 cm, W = 10 km) we need to explain the difference in $\bar{u}$ by a difference in $\Delta\sigma_d$ of about a factor of 15. Since the correlation between $\bar{u}$ and L is also good in these examples. we also need to argue that $\Delta\sigma_d$ determined L in these cases. On the other hand, it can be argued that the length of the 1966 earthquake was determined by the length of the gap between the rupture zone of the 1857 earthquake (or the

fault offset near Cholame) and the southern end of the creeping section of the San Andreas fault. Similarly, the 1906 earthquake filled the gap between the northern end of the creeping section at San Juan Bautista and the end of the fault at Cape Mendocino. If our argument that $\Delta\sigma_d$ determines L is true, then these latter observations are coincidences. Almost identical arguments can be made for many of the other earthquakes in our data set.

The third point is less an objection than a surprising consequence of this interpretation. The Hoei earthquake of 1707 ruptured about 500 km of the Nankai trough in Japan (Ando, 1975; Shimazaki and Nakata, 1980). The same plate boundary was ruptured twice subsequently, in two sets of delayed multiple events, the Ansei I and II events of 1854, and the Tonankai and Nankaido events of 1944 and 1946. In support of a time-predictable model of earthquake recurrence, Shimazaki and Nakata argued that the greater recurrence time between the first two sequences (147 years) and the second (91 years) is because the slip (and stress drop) were greater in 1707 than in either 1854 or 1946, the greater uplift at Muroto Point in 1707 (1.8 m) than in 1856 (1.2 m) or 1946 (1.15 m) being the evidence. The reason why this should happen is readily explained by the correlation between $\bar{u}$ and L. Thus the ratio of fault length of the Hoei and Ansei II earthquakes, 500 km/300 km = 1.7 can explain the ratio of uplift at Muroto Point, 1.8/1.2 = 1.5 and recurrence time, 147/91 = 1.6.

However, if this is interpreted as being due to a difference in dynamic stress drop, then one has to argue that a significant change in dynamic stress drop (50%) can occur on the same fault zone between successive earthquakes. One could argue that this could occur because the slip in one earthquake might change the relative position of asperities on the

fault. However, since the slip in an earthquake is about 10^{-5} L, this would mean that the gross frictional properties of the fault are controlled by asperities of dimensions on the order of 10^{-5} or less of the rupture dimensions. Since there will be a very large number of such small features, the average change between successive earthquakes would more likely be expected to be negligible.

In the above discussion we have created enough doubt about the applicability of the dynamic rectangular models to consider that they may be failing, in some fundamental way, to properly describe the physics of large earthquakes.

For a rupture propagating at a constant rupture velocity, v, the slip, for both circular and rectangular faults, is very close to [Day, 1979; Das, 1980, 1981]

$$u(x,y,t) = \dot{u}_o \left(t^2 - \frac{(x^2+y^2)}{v^2}\right)^{1/2} \qquad \frac{(x^2+y^2)^{1/2}}{v} \le t \le t_h \qquad (7)$$

·where x and y are measured relative to the point of rupture initiation. Equation (7) is the self-similar solution of Kostrov (1964). The asymptotic particle velocity, $\dot{u}_o$ which scales the slip is, (Kostrov, 1964; Dahlen, 1974)

$$\dot{u}_o = K\frac{\Delta\sigma_d}{\mu}\beta \qquad (8)$$

where K is a function of rupture velocity.

When the rupture reaches its final perimeter and stops, a healing wave propagates back into the rupture, arriving at time t_h. For $t > t_h$ slip decelerates and comes to a halt. The healing wave is not the stopping phase, which is a wave radiated in all directions from the tip of a

stopping crack (Savage, 1965). A stopping phase cannot physically stop the slip in these models because such a wave will lose energy with distance whereas the results of the models are independent of dimension. A healing wave must be interpreted as a wave that propagates into the interior of the rupture in an analogous way, and for analogous physical reasons, as the stopping of cars on a highway propagates up the stream of traffic. Causality restricts it to travel at a velocity slower than a stopping phase. Thus Madariaga (1976, p. 648) observed, "It appears as if a 'healing' wave propagates inward from the edge of the fault some time after the P and S stopping phases."

Since slip is terminated by the healing wave, the rise time and final slip at any point on the fault is determined by the distance to the nearest boundary (Day, 1979; Das, 1981). Therefore it is easy to see why mean slip on a rectangular fault should be controlled by the fault width.

A healing wave is the result of the boundary condition that u = 0 at the edges of the fault. If the models are poor representations of large earthquakes, the most likely problem is that these boundary conditions are unrealistic. The models are of rectangular faults embedded in an elastic whole space. The boundary condition u = 0 is imposed on all edges of the fault and healing waves thus propagate from each edge. Since large earthquakes rupture the free surface, slip is unconstrained there and a healing wave will not propagate from that edge. However even if an elastic half-space model were available, we would still expect slip to be width-dependent since it would be controlled by the healing wave from the base of the fault.

In large earthquakes the base of the fault is at the bottom of the seismogenic layer. A plausible explanation for the seismogenic depth is

that it is the result of a brittle-ductile transition. Thus a large earthquake cannot propagate to greater depth because the energy at the crack tip is dissipated in plastic deformation. A more realistic model then may be one in which the base of the fault is in a plastic, rather than elastic, region and therefore the condition u = 0 is no longer valid at that edge.

We illustrate in Figure 8 the difference between an elastic model and an elastic-plastic model. The most significant difference is that in the elastic-plastic model (Figure 8b) slip at the base of the fault may be allowed to be greater than zero as a result of plastic deformation in a zone surrounding the rupture tip. This is simply the equivalent, in shear, of the blunting of a crack tip that occurs in tensile crack propagation in ductile materia 3. The plastic deformation around the base of the fault smooths out the stress singularity associated with finite slip there, and will continue as long as slip continues. This may have the effect of inhibiting a healing wave from originating at the base, and if healing waves propagate only from the ends of the fault, slip and rise time will depend on fault length, not width.

No model is available with these boundary conditions but we can approximate one. If we make the approximation that slip stops abruptly with the arrival of the healing wave, then the final slip on the fault will be, from (7),

$$u(x,y) = \dot{u}_o (t_h^2 - \frac{(x^2+y^2)}{v^2})^{1/2} \tag{9}$$

which we can calculate. This is a 'quasidynamic' model (Boatwright, 1980), i.e., a kinematic model that simulates a dynamic model.

It can readily be shown for the circular case that (9) yields final slip values that are everywhere within 5% of that of the dynamic numerical models of Madariaga (1976) and Das (1980), and Day (1979) has shown that (9), when properly truncated, also yields a very good approximation to final slip in his rectangular models. We use it to simulate an elastic-plastic half-space model by simply assuming that no healing wave propagates from either the top or bottom of the fault.

The procedure we use is very similar to that used by Day (1979, pp. 23-26), and simply involves the calculation of t_h. We assumed $v = 0.9\beta$, for which the corresponding value of K is 0.81 (Dahlen, 1974), and that the velocity of the healing wave is $\sqrt{3}\beta$. In Figure 9 we show slip at the surface as a function of distance from the center of the fault for a bilateral case with $L/W = 4$. The mean slip is found to scale as

$$\bar{u} = \frac{1}{2}\frac{\Delta\sigma_d}{\mu}L \tag{10}$$

so this model would lead to the interpretation that the linear correlation between $\bar{u}$ and L that is observed means that the dynamic stress drop for large interplate earthquakes is approximately constant. Equating (10) with (4) we obtain $\Delta\sigma_d \approx 12$ bars and 7.5 bars for thrust and strike-slip earthquakes, respectively. Returning to Figure 4, the line drawn through the data is the prediction of this model for $\Delta\sigma_d = 10$ bars. Furthermore, in this model, where slip is unconstrained at top and bottom, static stress drop will also be a function of fault length, since the scale length that determines the strain change will be the fault length. The observation made earlier that $\Delta\sigma$ is a function of aspect ratio is due to the incorrect use of equation (2) to calculate it. According to this model, $\Delta\sigma$ is also approximately constant for these earthquakes.

DISCUSSION

The observation that slip increases with fault length in large earthquakes poses severe consequences when viewed in the light of dynamic rupture models. In conventional dynamic models (W models), slip is determined by fault width, rather than length. These models can only be reconciled with the observations if it is assumed that the dynamic stress drop determines the fault length, and the several major objections to this possibility were detailed earlier. With different assumptions concerning the boundary conditions at the base of the fault, it may be possible to construct a dynamic model in which slip depends on fault length (L model). This model avoids the objections raised to the W model but is based on a speculative, although not entirely ad hoc, assumption concerning the boundary conditions.

Furthermore, severe constraints are placed on L models from the geodetic data obtained for the 1906 San Francisco earthquake. The simplest form of L model is one in which slip is totally unconstrained at the base of the fault. If this were the case, strain release would extend out to distances comparable to fault length, rather than depth, but as Brune (1974) has pointed out, the strain release in 1906 was concentrated within a few tens of km from the fault. From angle changes in the Pt. Arena triangulation network [angle $\dagger$ from Thatcher (1975, Fig. 4)] one can estimate a strain drop of 8×10^{-5} within 12 km of the fault, a figure somewhat more consistent with a W model than an L model. Thus if L models are relevant, they must be models in which slip is only <u>partially</u> constrained at the base of the fault. In the absence of numerical modeling of

this type, one can't tell if this type of model will result in L scaling or hybrid scaling intermediate to the L and W extremes.

These L and W models represent, in many respects, opposite extremes concerning the mechanism of large earthquakes and so it is useful to discuss the contrasting way in which they scale. For earthquakes in which L < 2W, the models are indistinguishable in their gross manifestations. In Figure 10 we schematically show a comparison between an earthquake of dimensions about L = 2W and one of the same width but about 15 times longer. Specifically, this might be a comparison of the 1966 Parkfield earthquake, say, and the 1906 San Francisco earthquake.

On the left of the figure we show a snapshot of slip on the fault during the smaller earthquake. We only show the part that is actually slipping during the snapshot. We also show the time history of slip at some representative point. For simplicity, it is simply shown as a ramp with a rise time, t_R. On the right is shown the predictions of the two models for the longer earthquake.

In a bilateral case, as shown, the W model predicts that the slipping portion of the fault splits into two patches of length $\sim$ W that propagate away from each other at a velocity 2v as they sweep over the fault surface. Since the rise time $t_R \simeq W/2\beta$, remains the same but the slip is fifteen times greater, the dynamic stress drop, and hence particle velocity, must be fifteen times greater.

In the L model, the rupture sweeps out over the fault as an expanding patch, with slip continuing within its boundaries until after the final dimensions are reached. In that model, the dynamic stress drop and particle velocities are the same as in the smaller event, but the rise time, $t_R \simeq L/2\beta$ is much longer.

In terms of predicting the strong ground motions for a 1906 size earthquake, say, from observed ground motions for a 1966 size earthquake, the difference between the W and L model is critical. The W model would predict that the average particle velocities would be much higher and the duration would be about the same. The L model would predict nearly the opposite.

Suppose we start with a square rupture of width W_o and consider how peak particle velocity, $\dot{u}_p$, and the asymptotic particle velocity, $\dot{u}_o$, increase for ruptures of greater length. For a square rupture with dynamic stress drop, $\Delta\sigma_d^S$, the maximum value of $\dot{u}_p$ and the asymptotic value $\dot{u}_o$ will be

$$\dot{u}_p^S \propto \Delta\sigma_d^S \sqrt{W_o}$$

and

(11)

$$\dot{u}_o^S \propto \Delta\sigma_d^S$$

Using the W model, for a rupture of width W_o and length $L > W_o$, the stress drop will have to be greater by the ratio

$$\frac{\Delta\sigma_d^W}{\Delta\sigma_d^S} = \frac{L}{W_o}$$

so that

$$\dot{u}_p^W \propto \Delta\sigma_d^S \frac{L}{W_o} \sqrt{W_o}$$

and

(12)

$$\dot{u}_o^W \propto \Delta\sigma_d^S \frac{L}{W_o}$$

For the L model, stress drop is the same but the scale length that determines the maximum peak velocity becomes L rather than W, so that

$$\dot{v}_p^L \propto \Delta\sigma_d^S \sqrt{L}$$

and

(13)

$$\dot{u}_o^L \propto \Delta\sigma_d^S$$

Comparing (12) and (13), the two models differ in the ratios

$$\frac{\dot{u}_p^L}{\dot{u}_p^W} = \sqrt{\frac{W_o}{L}}$$

and

(14)

$$\frac{\dot{u}_o^L}{\dot{u}_o^W} = \frac{W}{L}$$

So that with a W model, from (12), both peak and asymptotic velocities for a 1906 type earthquake would be about 15 times greater than for the Parkfield earthquake. For the L model, from (13), the peak velocities would at maximum be about $\sqrt{15}$ greater for a 1906 than a 1966 event, but the asymptotic value would be the same.

These remarks, of course, apply only to the simple case of a smoothly propagating rupture. Any heterogeneity will produce local high frequency variations in the velocities. However, they serve to point out the importance of determining if large earthquakes are better described by an L model or W model or by some intermediate case, if such can exist.

ACKNOWLEDGEMENTS

REFERENCES

Abe, K. (1975). Reliable estimation of the seismic moment of large earthquakes, J. Phys. Earth, 23, 381-390.

Aki, K. (1967). Scaling law of seismic spectrum, J. Geophys. Res., 72, 1217-1231.

Aki, K. (1972). Earthquake mechanism, Tectonophysics, 13, 423-446.

Aki, K. (1980). Re-evaluation of stress drop and seismic energy using a new model of earthquake faulting, in Source Mechanism and Earthquake Prediction, p. 23-50, Edit. Centre Nat. Recherche Sci., Paris.

Ambraseys, N. (1970). Some characteristics of the Anatolian fault zone, Tectonophysics, 143-165.

Archuleta, R J. (1976). Experimental and numerical three dimensional simulations of strike-slip earthquakes, Ph.D. thesis, Univ. of Calif., San Diego.

Archuleta, R. J., and S. M. Day (1980). Dynamic rupture in a layered medium: the 1966 Parkfield earthquake, Bull. Seismol. Soc. Amer., 20, 671-689.

Ando, M. (1975). Source mechanisms and tectonic significance of historic earthquakes along the Nankai trough, Japan, Tectonophysics, 27, 119-140.

Boatwright, J. (1980). A spectral theory for circular seismic sources; simple estimates of source dimension, dynamic stress drop, and radiated seismic energy, Bull. Seismol. Soc. Amer., 70, 1-27.

Bonilla, M. G., and J. M. Buchanan (1970). Interim report on worldwide historic surface faulting, U. S. Geol. Surv. Open-File Rept., Washington, D.C.

Brune, J. N. (1974). Current status of understanding quasi-permanent fields associated with earthquakes, EOS, Trans. AGU, 55, 820-827.

Dahlen, F. A. (1974). On the ratio of P-wave to S-wave corner frequencies for shallow earthquake sources, Bull. Seismol. Soc. Amer., 64, 1159-1180.

Das, S. (1980). A numerical method for determination of source-time functions for general three-dimensional rupture propagation, Geophys. J. R. Astron. Soc., 62, 591-604.

Das, S. (1979). Three-dimensional spontaneous rupture propagation and implications for the earthquake source mechanism, Geophys. J. R. Astron. Soc., in press.

Day, S. (1979). Three-dimensional finite difference simulation of fault dynamics, Final Rept., NAS2-10459, 71 pp., Systems, Science and Software, La Jolla, Calif.

Geller, R. J. (1976). Scaling relations for earthquake source parameters and magnitudes, Bull. Seismol. Soc. Amer., 66, 1501-1523.

Hanks, T. C. (1977). Earthquake stress drops, ambient tectonic stress, and stresses that drive plate motions, Pure Appl. Geophys., 115, 441-458.

Kanamori, H., and D. L. Anderson (1975). Theoretical basis of some empirical laws of seismology, Bull. Seismol. Soc. Am., 65, 1073-1096.

Kostrov, B. V. (1964). Selfsimilar problems of propagation of shear cracks, J. Appl. Math. Mech., 28, 1077-1087.

Madariaga, R. (1976). Dynamics of an expanding circular fault, Bull. Seismol. Soc. Amer., 66, 639-666.

Savage, J. C. (1965). The stopping phase on seismograms, Bull. Seismol. Soc. Amer., 55, 47-58.

Shimazaki, K., and T. Nakata (1980). Time-predictable recurrence model for large earthquakes, Geophys. Res. Lett., 7, 279-282.

Sieh, K. (1978). Slip along the San Andreas fault associated with the great 1857 earthquake, Bull. Seis. Soc. Amer., 68, 1421-1448.

Slemmons, D. B. (1977). State of the art for assessing earthquake hazards in the United States, Faults and earthquake magnitudes, U.S. Army Eng. Waterway Exp. Sta., Vicksburg, Miss., pp. 229, 1977.

Sykes, L. R., and R. C. Quittmeyer (1981). Repeat times of great earthquakes along simple plate boundaries, Third Maurice Ewing Symposium on Earthquake Prediction, 4, edited by D. W. Simpson and P. G. Richards, AGU, Washington, D.C.

Thatcher, W. (1975). Strain accumulation and release mechanism of the 1906 San Francisco earthquake, J. Geophys. Res., 80, 4862-4872.

Thatcher, W., and T. Hanks (1973). Source parameters of southern California earthquakes, J. Geophys. Res., 78, 8547-8576.

TABLE 1

PARAMETERS OF LARGE INTERPLATE EARTHQUAKES
(AVERAGED FROM SYKES AND QUITTMEYER (1981))

No.	Date	Location	Mo 10^{27} dyne-cm	L km	W km	L/W	$\bar{u}$ cm	$\Delta\sigma$ bars
			Strike-Slip Earthquakes					
1.	10 Jul 1958	SE Alaska	4.3	350	12	29	325	26
2.	9 Jan 1857	S. California	7	380	12	32	465	36
3.	18 Apr 1906	San Francisco	4	450	10	45	450	44
4.	19 May 1940	Imperial Va., Ca.	0.23	60	10	6	125	13
5.	27 Jun 1966	Parkfield, Calif.	0.03	37	10	4	30	4
6.	9 Apr 1968	Borrego Mtn, Ca.	0.08	37	12	3	25	3
7.	15 Oct 1979	Imperial Va., Ca.	0.03	30	10	3	30	4
8.	4 Feb 1976	Guatemala	2.6	270	15	18	150	9
9.	16 Oct 1974	Gibbs F. Z.	0.45	75	12	6	170	14
10.	26 Dec 1939	Ercincan, Turkey	4.5	350	15	23	285	18
11.	20 Dec 1942	Erbaa Niksar, Turkey	0.35	70	15	5	112	8
12.	1 Feb 1944	Gerede-Bolu, Turkey	2.4	190	15	13	275	18
13.	18 Mar 1953	Gönen-Yenice, Turkey	0.73	58	15	4	280	21
14.	22 Jul 1967	Mudurnu, Turkey	0.36	80	15	5	100	7
			Thrust Earthquakes					
15.	6 Nov 1958	Etorofu, Kuriles	44	150	70	2.1	840	37
16.	13 Oct 1963	Eruppu, Kuriles	67	275	110	2.5	445	12
17.	16 May 1968	Tokachi-oki, Japan	28	150	105	1.4	355	10
18.	11 Aug 1969	Shikotan, Kuriles	22	230	105	2.2	180	5
19.	17 Jun 1973	Nemuro-oki, Japan	6.7	90	105	0.86	140	5
20.	4 Nov 1952	Kamchatka	350	450	175	2.6	890	14
21.	28 Mar 1964	Prince Wm Sound, Alaska	820	750	180	4.2	1215	18
22.	4 Feb 1965	Rat Island, Aleutians	125	650	80	8.1	480	10
23.	10 Jan 1973	Colima, Mexico	3	85	65	1.3	110	5
24.	29 Nov 1978	Oaxaco, Mexico	3	80	70	1.1	110	5
25.	22 May 1960	S. Chile	2000	1000	210	4.8	1900	21
26.	17 Oct 1966	C. Peru	20	80	140	0.6	360	12

FIGURE CAPTIONS

Figure 1.   Plot of log LW^2 vs. log M_o for the large intraplate earthquakes from the data set of Sykes and Quittmeyer (1981). The lines of slope 1 are constant stress drop lines, assuming $C = 0.6$ for the thrust events, and 0.3 for the strike-slip events.

Figure 2.   A plot of mean slip, $\bar{u}$, vs. fault length for the strike-slip events. The line drawn through the data has a slope of 1.25×10^{-5}. Numbers are references to Table 1.

Figure 3.   The same as Figure 2, for the thrust events. The slope of the line is 2×10^{-5}.

Figure 4.   A plot of log L^2W vs. log M_o. The line drawn through the data has a slope of 1, for reference.

Figure 5.   Stress drop plotted vs. aspect ratio for the strike-slip earthquakes.

Figure 6.   Stress drop vs. aspect ratio for the thrust earthquakes. Event 22 is an oblique slip event for which stress drop was calculated based only on the dip slip component and is hence underestimated. Event 15 is an anomalously deep event in the Kuriles (Sykes and Quittmeyer, 1981).

Figure 7.   Schematic representation of two models of large earthquakes. In A, it is represented by rupture in an elastic half-space. The boundary condition at the base of the rupture is u = 0. In B, the rupture penetrates a ductile region. At the base u > 0, which is accommodated by plastic deformation in a zone surrounding the rupture tip.

Figure 8.   Surface slip as a function of distance along the fault plane for two representative strike-slip earthquakes of similar width but different depth. Data for the Mudurnu earthquake is from Ambraseys (1969) and for the Ft. Tejon earthquake from Sieh (1978).

Figure 9.   Dimensionless slip, u' vs. length, L', at the free surface from the center to the end of the fault. The model is a quasidynamic one that simulates a dynamic model with boundary conditions similar to those shown in Figure 7b, as described in the text. The normalization relations are $u = \frac{\Delta\sigma_d}{\mu}Wu'$ and $L = WL'$. The case shown is bilateral with aspect ratio 4.

Figure 10.   A schematic diagram to illustrate the contrasting way in which a model in which width determines the slip (W model) scales with length as compared to a length dependent model (L model).
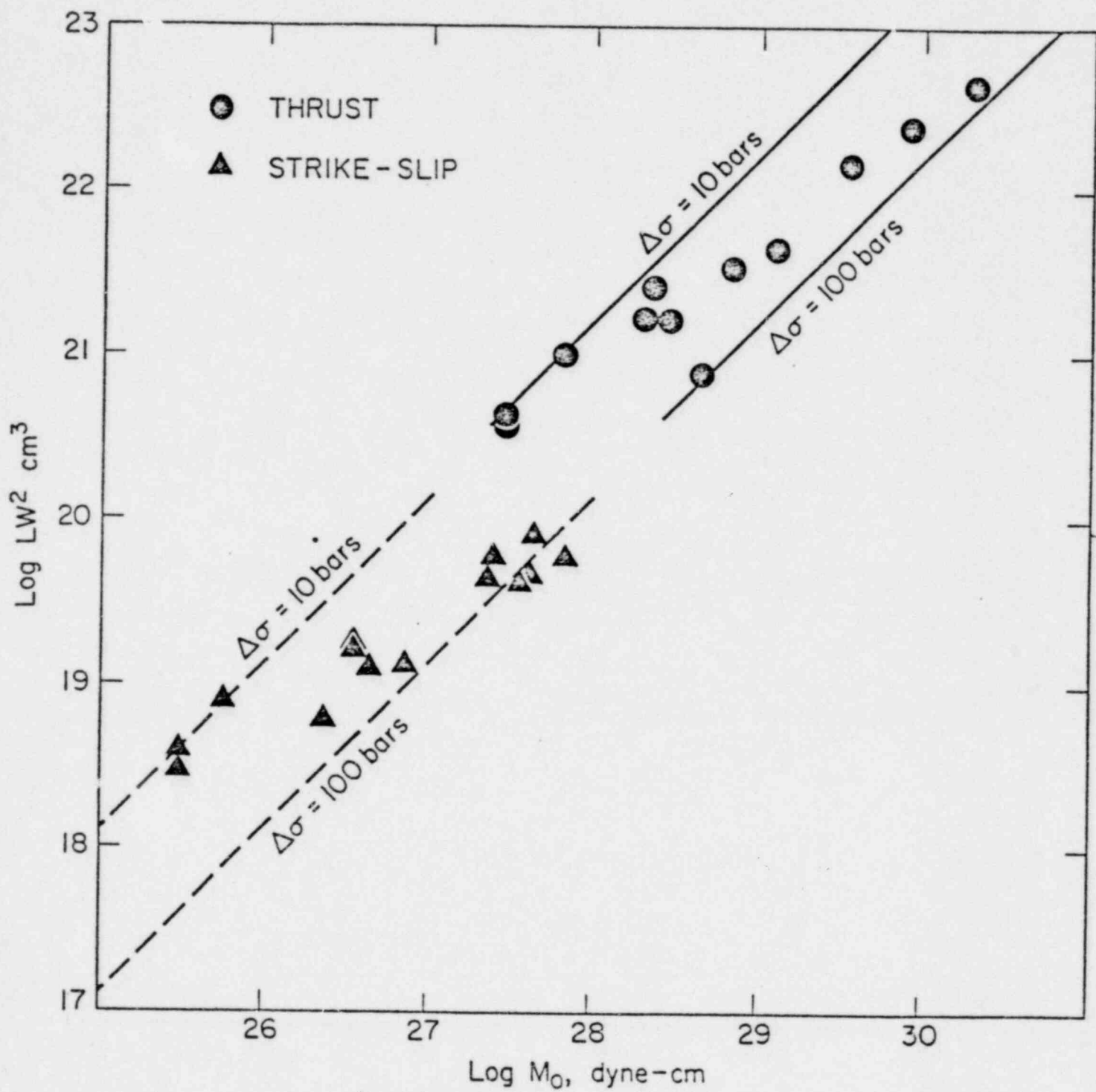
Figure 1
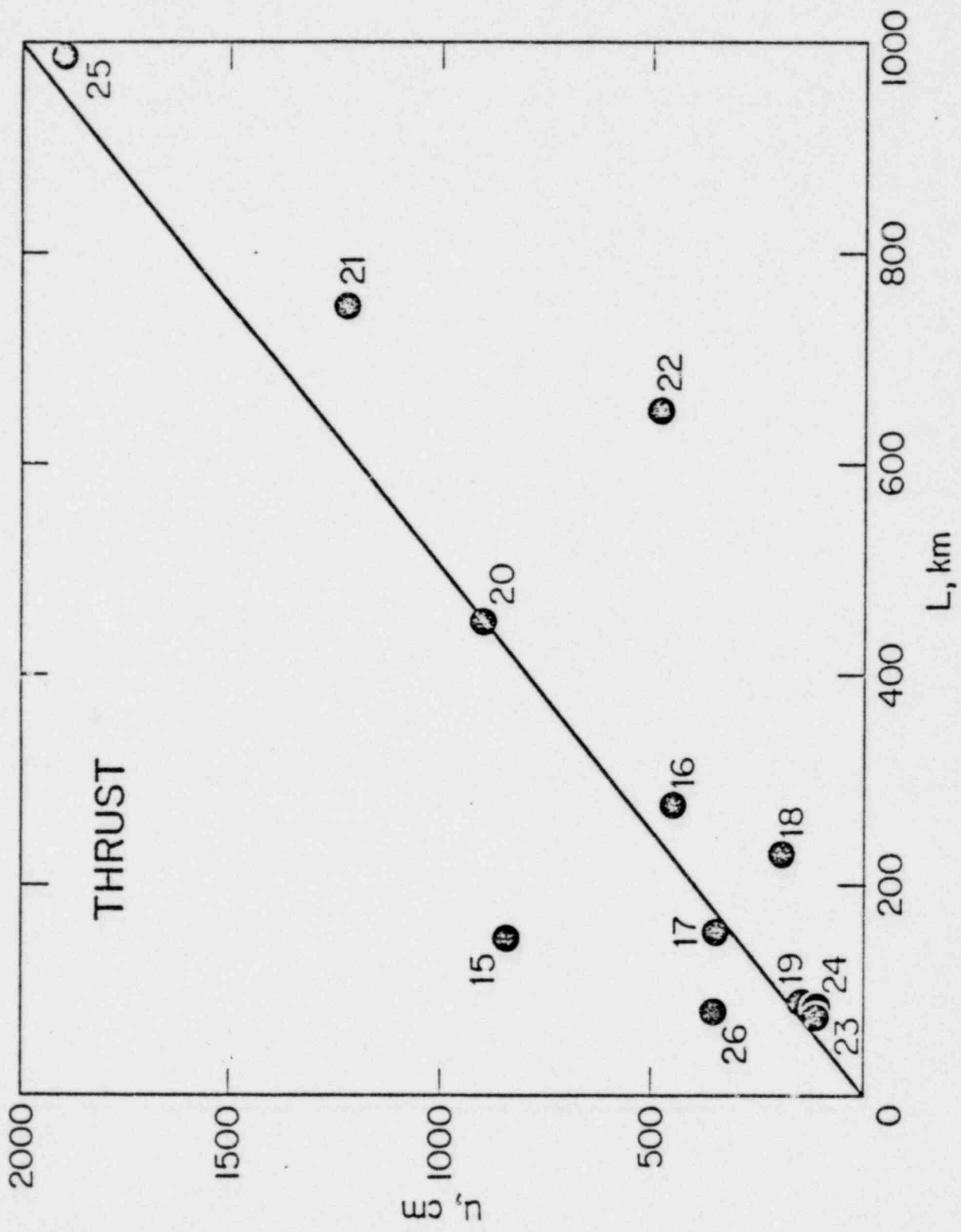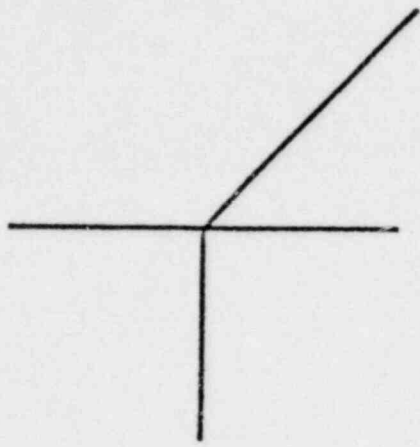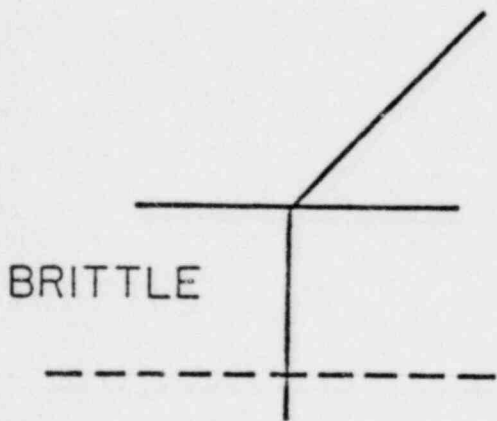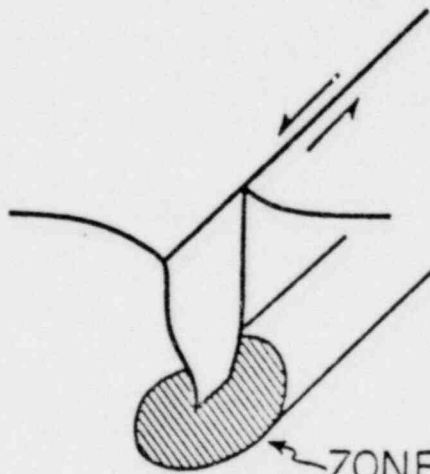
Figure 3

Figure 2

Figure 4

L/W
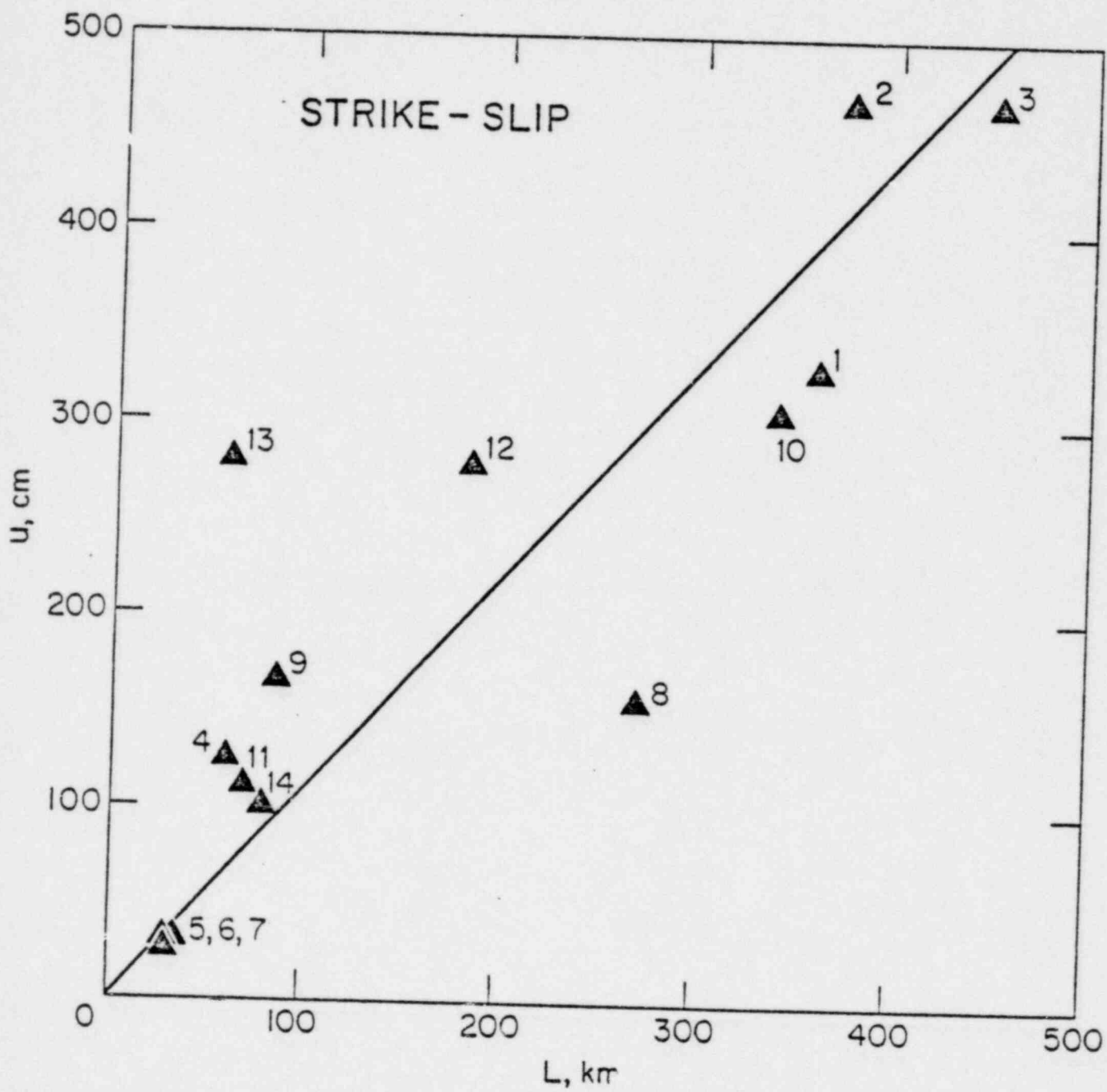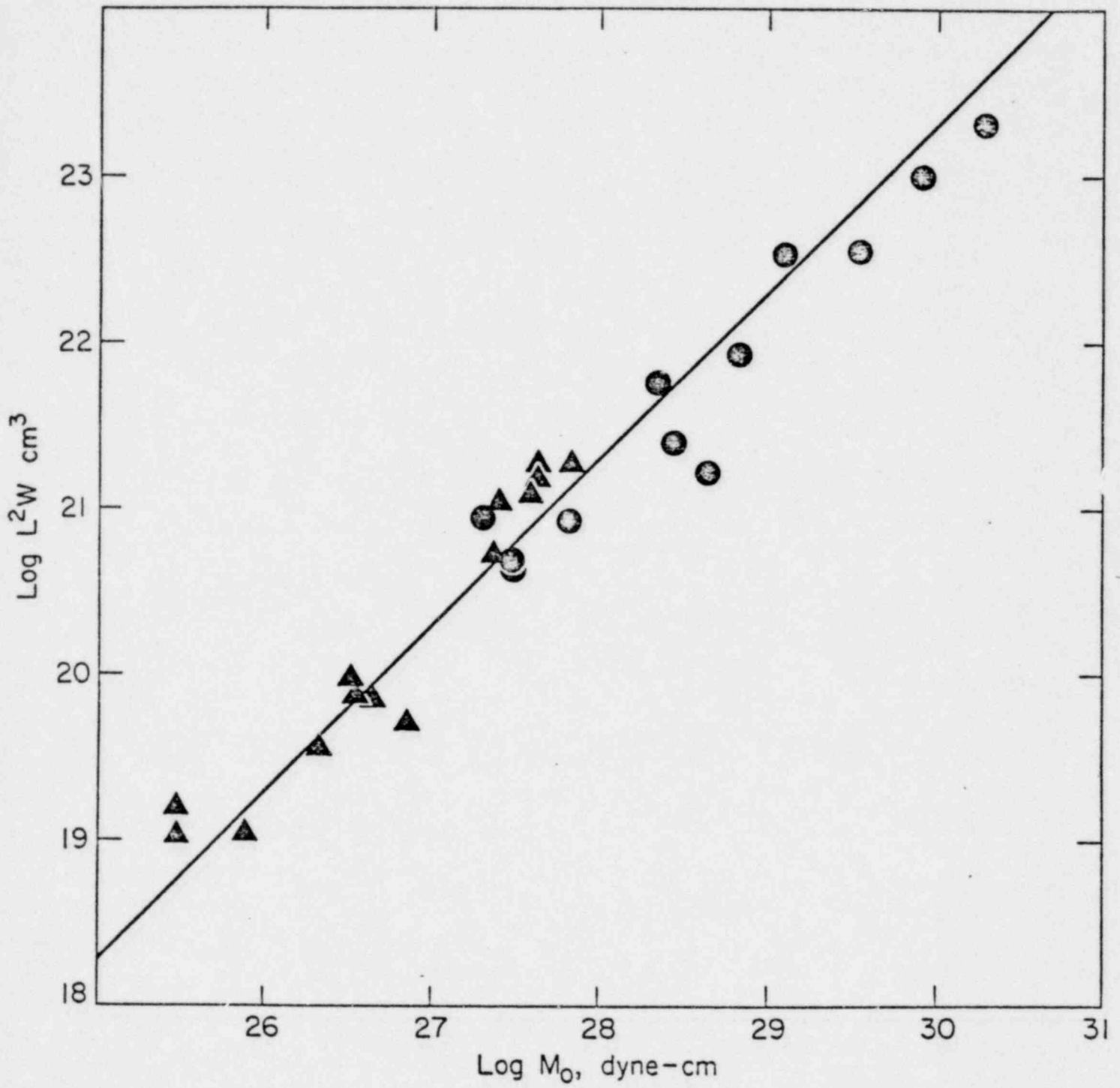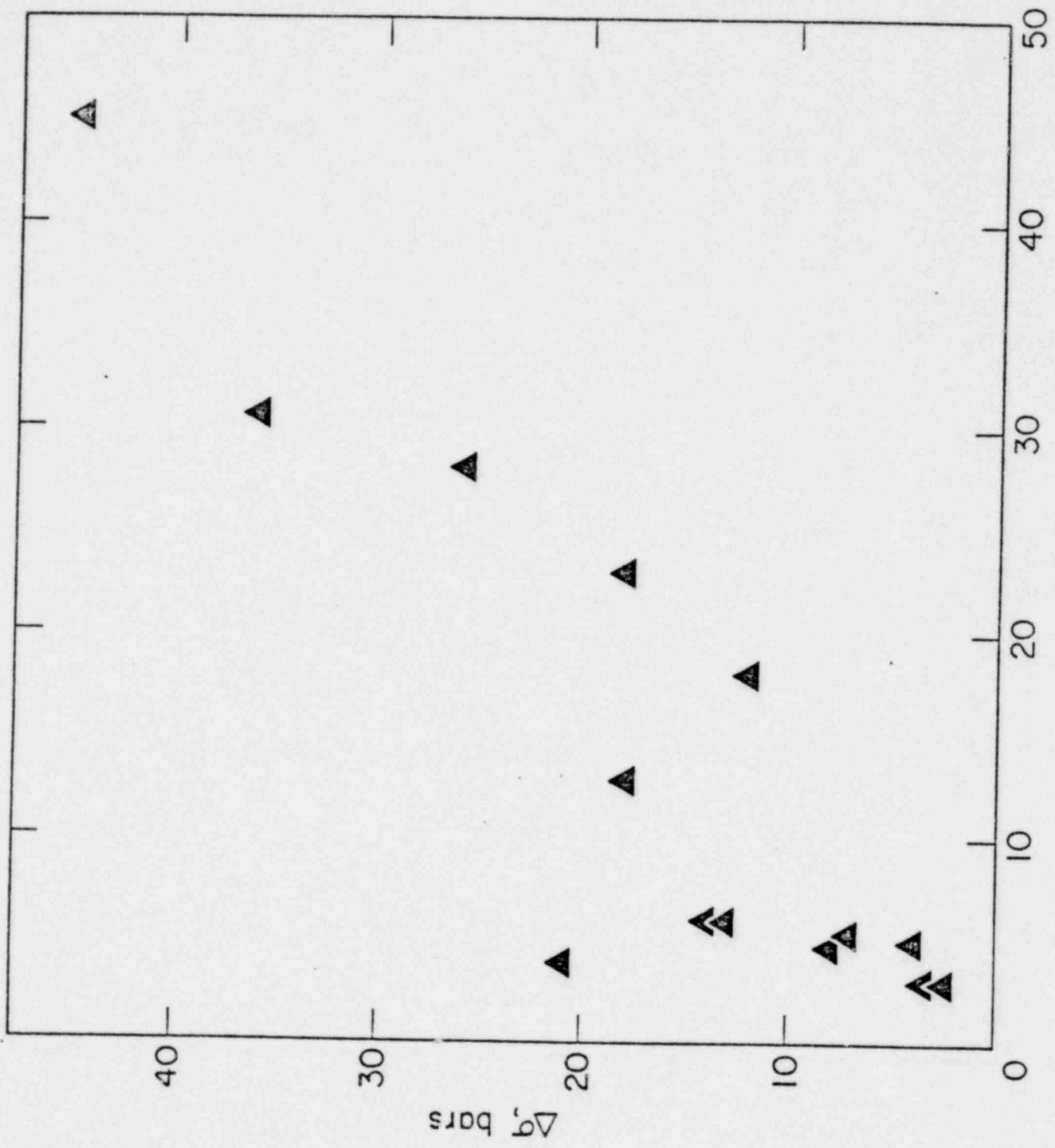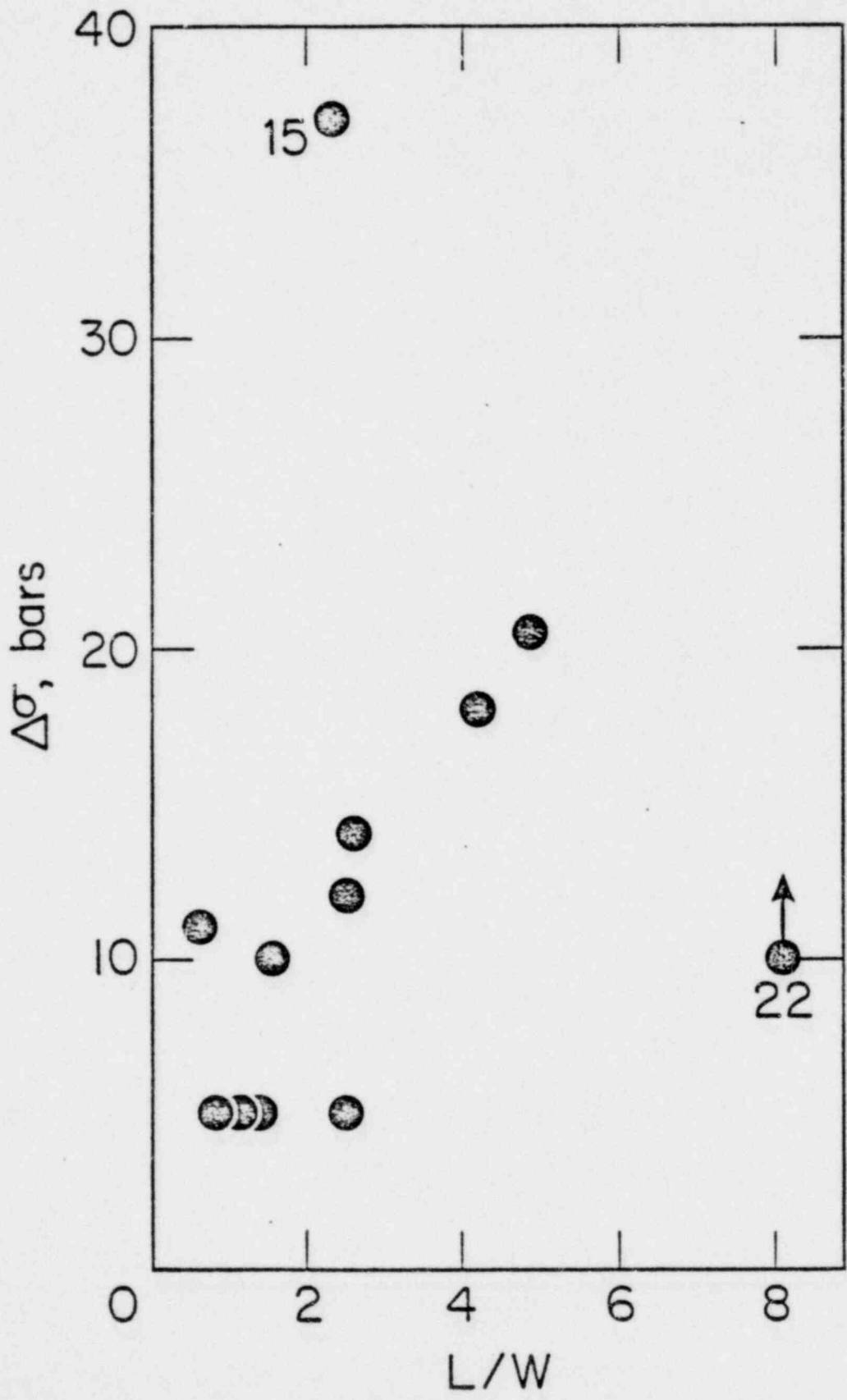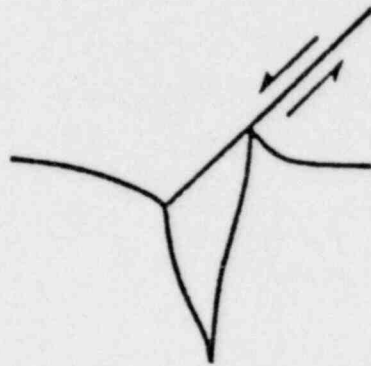
Figure 5

Figure 6
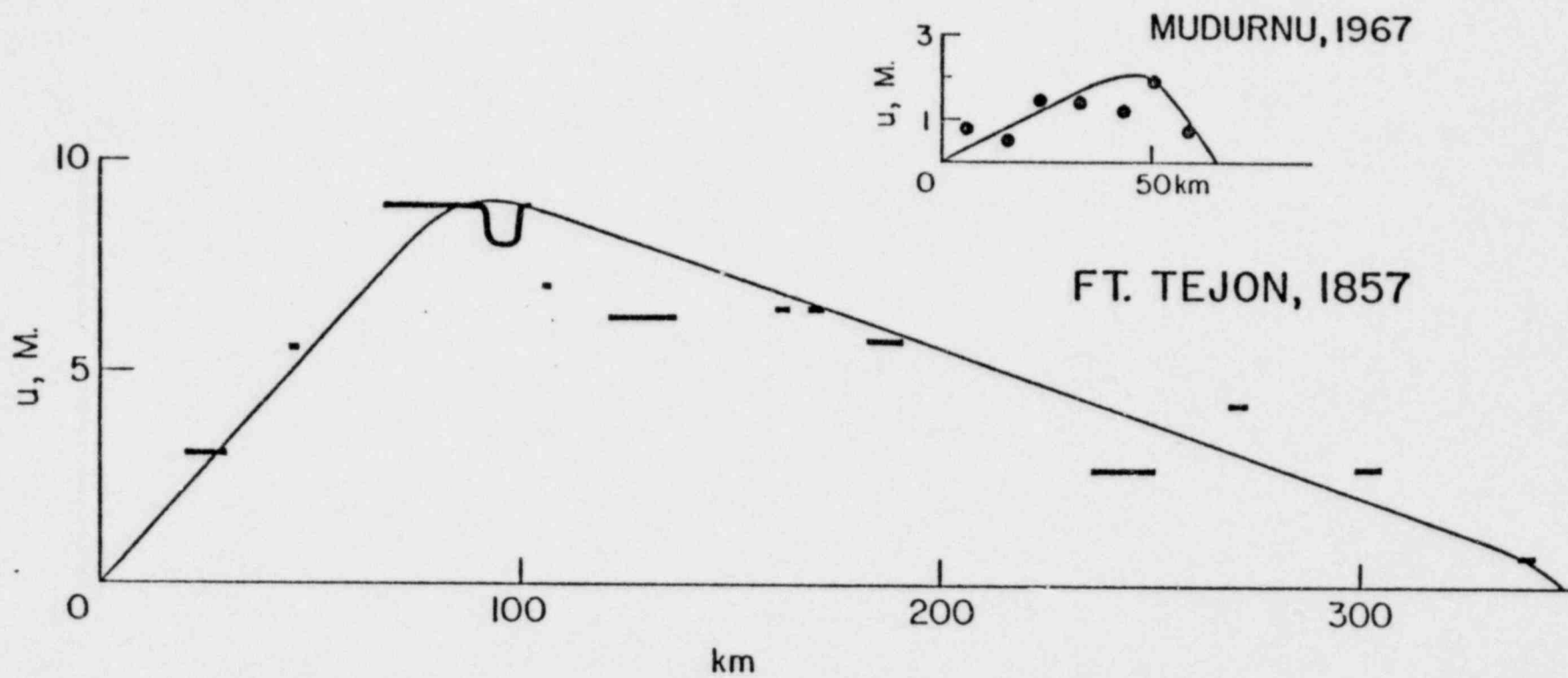
BRITTLE

DUCTILE

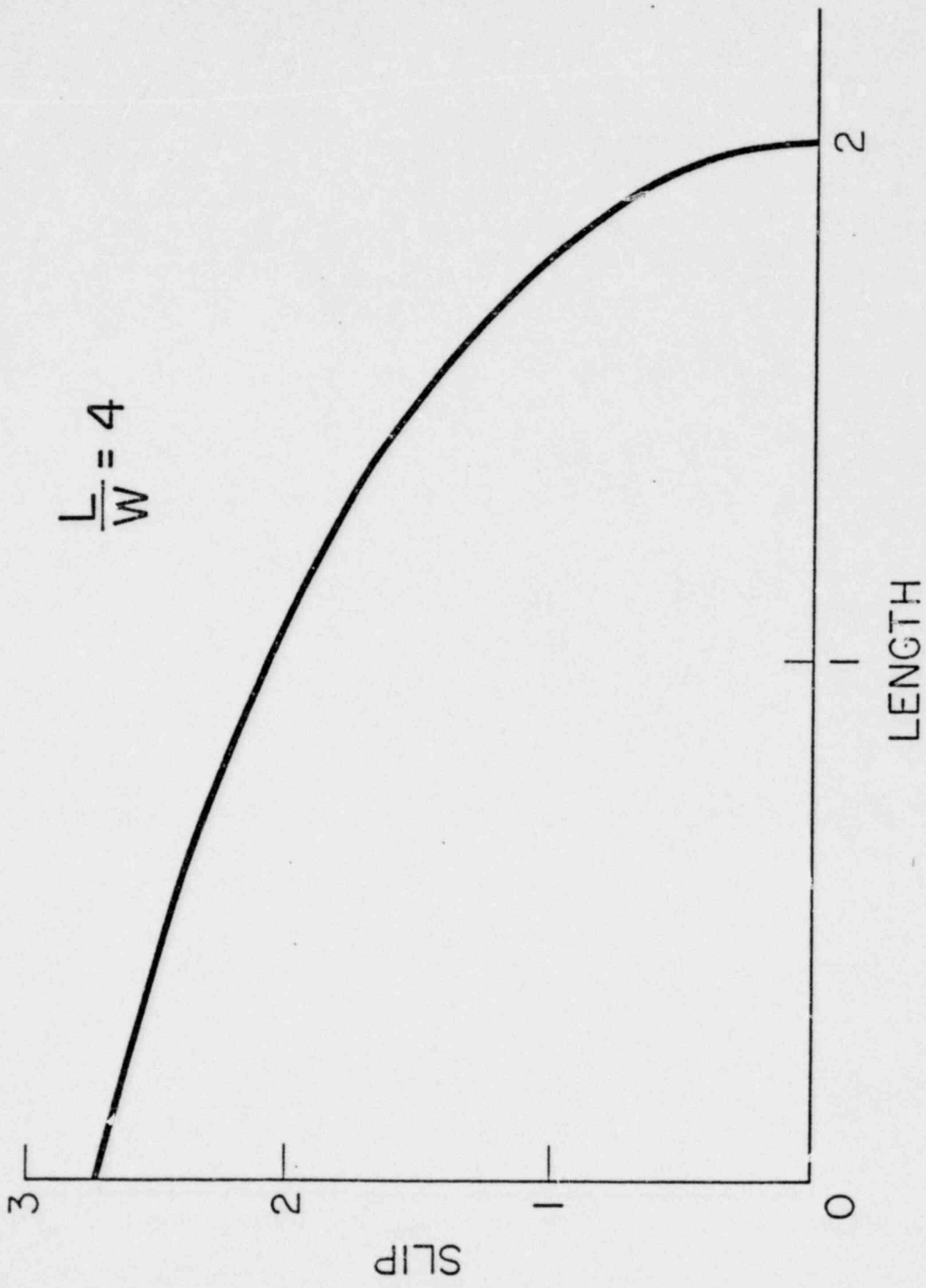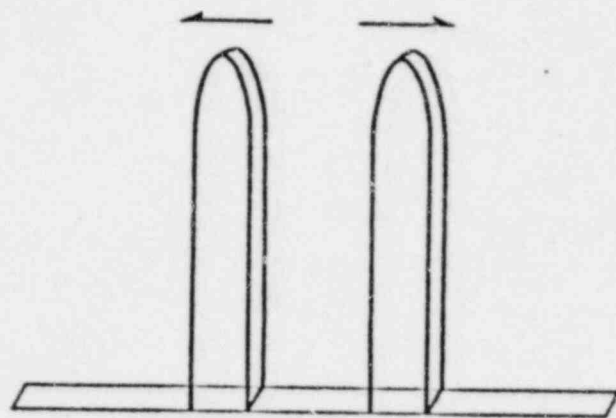ZONE OF
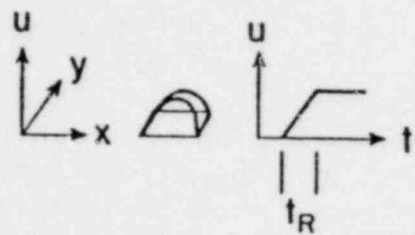PLASTIC DEFORMATION

A

B

Figure 7

Figure 8
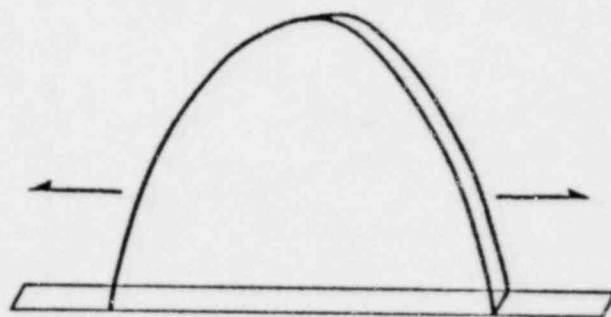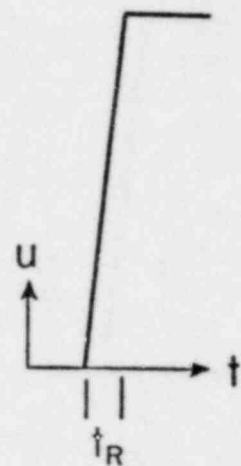
Figure 9

W – MODEL

L – MODEL
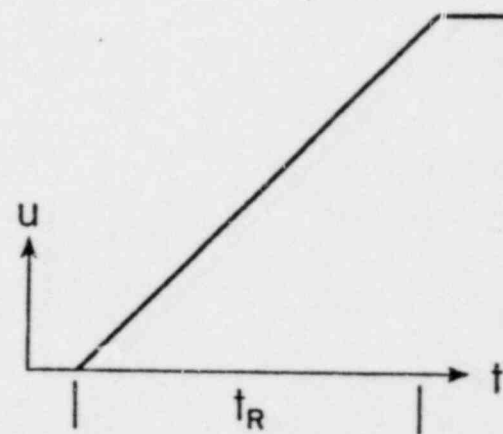
Figure 10

UNITED STATES OF AMERICA
NUCLEAR REGULATORY COMMISSION

BEFORE THE ATOMIC SAFETY AND LICENSING APPEAL BOARD

```
                              )
In the Matter of:            )
                              )
PACIFIC GAS & ELECTRIC       )     Docket Nos. 50-275 O.L.
  COMPANY                    )                 50-323 O.L.
  (Diablo Canyon Nuclear     )
Power Plant, Units 1 & 2     )
                              )
                              )
```

CERTIFICATE OF SERVICE

I hereby certify that on this 24th day of May, 1981,
I have served copies of the foregoing MOTION TO REOPEN THE RECORD
by mailing them through the U.S. Mail, first-class, postage pre-
paid, to those persons listed below, except those designated by
an asterisk on whom service was made by messenger on May 26, 1981.

* Richard S. Salzman,
    Chairman
Atomic Safety & Licensing
  Appeal Board
U.S. Nuclear Regulatory
  Commission
4350 East West Highway
Bethesda, Maryland   20014

* Dr. W. Reed Johnson
Atomic Safety & Licensing
  Appeal Board
U.S. Nuclear Regulatory
  Commission
4350 East West Highway
Bethesda, Maryland   20014

* Dr. John H. Buck
Atomic Safety & Licensing
  Appeal Board
U.S. Nuclear Regulatory
  Commission
4350 East West Highway
Bethesda, Maryland   20014

John F. Wolf
  Chairman
Atomic Safety & Licensing
  Board
3409 Shepherd Street
Chevy Chase, Maryland   20015

Docket & Service Section
Office of the Secretary
U.S. Nuclear Regulatory
  Commission
Washington, D.C.   20555

William J. Olmstead, Esq.
Edward G. Ketchen, Esq.
'Lucinda Low Swartz
Charles A. Barth
Office of the Executive Legal
  Director - BETH 042
U.S. Nuclear Regulatory
  Commission
Washington, D.C.   20555

Mrs. Elizabeth Apfelberg
c/o Nancy Culver
192 Luneta Drive
San Luis Obispo, CA   93401

Mr. Frederick Eissler
Scenic Shoreline Preservation
· Conference, Inc.
4623 More Mesa Drive

Sandra A. Silver
1760 Alisal Street
San Luis Obispo, CA   93401

Malcolm H. Furbush, Esq.
Vice President and
  General Counsel
Philip A. Crane, Esq.
Douglas A. Oglesby
Pacific Gas & Electric Company
31st Floor
77 Beale Street, Room 3127
San Francisco, CA   94106

Gordon Silver
1760 Alisal Street
San Luis Obispo, CA   93401

Joel Reynolds
John Phillips, Esq.
Center For Law In-
The Public Interest
10203 Santa Monica Boulevard
Fifth Floor
Los Angeles, CA   90067

Bruce Norton, Esq.
3216 N. Third Street
Suite 202
Phoenix, Arizona 85012

Janice E. Kerr, Esq.
Lawrence Q. Garcia, Esq.
California Public Utilities
  Commission
5346 State Building
350 McAllister Street
San Francisco, California   94102

Arthur C. Gehr, Esq.
Snell & Wilmer
3100 Valley Center
Phoenix, Arizona 85073

David S. Fleischaker, Esq.